Ionization potential depression and Mechanical-electric coupling in plasma

Yuanjie Huang

Mianyang, *Sichuan province*, *People's Republic of China*

*Corresponding author's E-mail: hyj201207@163.com

Abstract

The ionization potential depression (IPD) is crucial for understanding the ionization processes of atoms and ions in plasmas. Many efforts have been devoted to exploring the temperature and the density dependence of IPD, leading to the development of models such as the Ecker-Kröll (EK) and Stewart-Pyatt (SP) models. However, these models fail to explain the plasma spectroscopy observed during laser nitriding process. To address the problem, the present study introduces a novel IPD model and the concept of mechanical-electric coupling (MEC) for the plasma. The MEC is important as it can influence a multitude of physical properties, including the diffusion of ionized electrons, Debye screening and the ionized electron pressure. The IPD model proposed herein is constructed based on spherical wave functions for the ionized electrons. It has been shown that this IPD model aligns well with both experimental spectroscopic data and the experimental IPD values for ions across various charge states. The integration of MEC with the IPD model may culminate in the formulation of an equation of state that is in concordance with experimental observations of the plasma behaviors. Overall, the MEC and IPD model proposed in this study could be instrumental for comprehending the ionization processes and the diverse properties of plasmas.

keywords: ionization potential depression; mechanical-electric coupling; plasma; electron chemical potential; equation of state;

1. Introduction

The ionization of atoms and the consequent formation of plasma is an important topic in diverse scientific areas, including astrophysics, magnetic confinement fusion, laser inertial confinement fusion and the laser nitriding of the active metals. The ionization of atoms and ions at elevated temperatures is typically characterized by the well-known Saha equation [1, 2, 3]. Within the equation, the ionization potential depression (IPD) is considered as a crucial factor and is widely believed to be significantly influenced by the Debye screening inherent to the plasma [2, 4, 5, 6, 7, 8, 9, 10]. As a result, several important models, such as the Ecker-Kröll (EK) model [20 6] and the Stewart-Pyatt (SP) model [21 7], along with various theoretical approaches [8, 9, 11], have been formulated. These models have been extensively applied to elucidate the ionization process [12, 13, 14, 15]. And they predict a small IPD value so that nitrogen (N) atoms are seldom ionized during the laser nitriding process. However, the prediction starkly contrasts with the experimental findings which demonstrate that nitrogen (N) atoms are completely ionized to form N^+ ions within the plasma, as detailed in subsequent sections.

Furthermore, in-situ laser-induced breakdown spectroscopy (LIBS) from both previous [16] and current studies indicates that the central wavelengths of the spectral peaks emitted by ions and atoms remain largely invariant as the plasma evolves. These experimental observations can imply that the energy levels of the bound electrons in the outer shells of ions and atoms do not fluctuate with plasma evolution. In addition, the characteristic X-ray fluorescence [12, 13, 15] and

ultraviolet spectra of the plasma [17, 18] show that the central wavelengths of spectral peaks emitted by the relevant ions also remain unchanged with plasma evolution. These experimental findings collectively suggest that the energy levels of bound electrons in the inner shells of ions and atoms are not altered by the dynamic electromagnetic environment of the plasma. Collectively, the experimental outcomes definitively indicate that the all the energy levels of bound electrons for the specific ions and atoms remain unaltered, notwithstanding the intricate evolution of the plasma. However, these results are at odds with the conventional plasma theory, which often incorporates the Debye screening effect and thereby typically predicts a noticeable shift in bound electron energy levels [9, 10, 19] as the density and temperature of the plasma varies over the time.

To reconcile the discrepancies between the experimental observations and the conventional plasma theory, an IPD model and a concept of mechanical-electric coupling (MEC) for the plasma were proposed in this study. And they were employed to investigate both the ionization of bound electrons and the diverse physical properties of the plasma.

2. Experimental methods

The experimental setup was detailed in the related work [16]. The metal targets were high-purity niobium (Nb content>99.95%, purchased from Xinwang scientific research metal material). The targets were put in a pressure container. The pressure container was first evacuated to a residual air pressure 2×10^{-3} *Pa* and then filled with high-purity

nitrogen gas (N_2 content> 99.999%, phased from Sichuan Runtai Special Gas Co. Ltd.). The nitrogen gas pressure in the container was controlled to be 1 atm.

The in situ laser-induced breakdown spectroscopy (LIBS) experiments were carried out and its detailed introduction was given by the previous work [17, 20]. The data collection duration was 20 *ns*. By altering the delay time of the LIBS system, the delay time dependence of LIBS for the plasma can be obtained. In the experiments, the laser energy density illuminated at niobium surface was designed to be 10.4 J/cm^2 and 20 J/cm^2, respectively.

3. Results and discussion

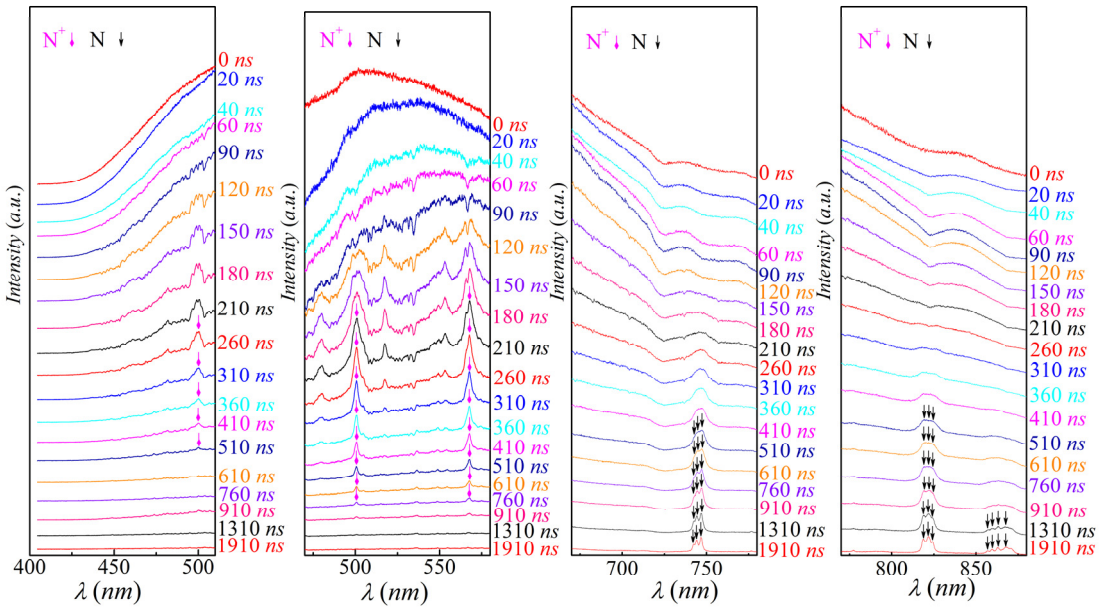

Figure 1 Delay time dependence of the in situ laser-induced breakdown spectroscopy (LIBS) created by the laser irradiation on the niobium in nitrogen gas with the illumination energy density 20 J/cm^2.

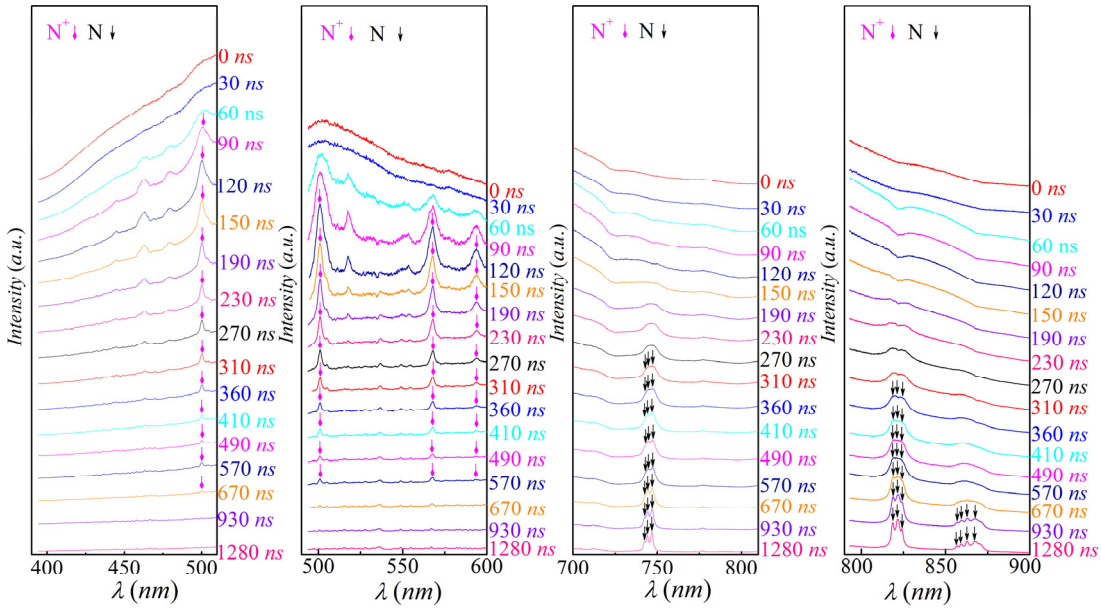

Figure 2 Delay time dependence of the in situ laser-induced breakdown spectroscopy (LIBS) created by the laser irradiation on the niobium in nitrogen gas with the illumination energy density 10.4 J/cm^2.

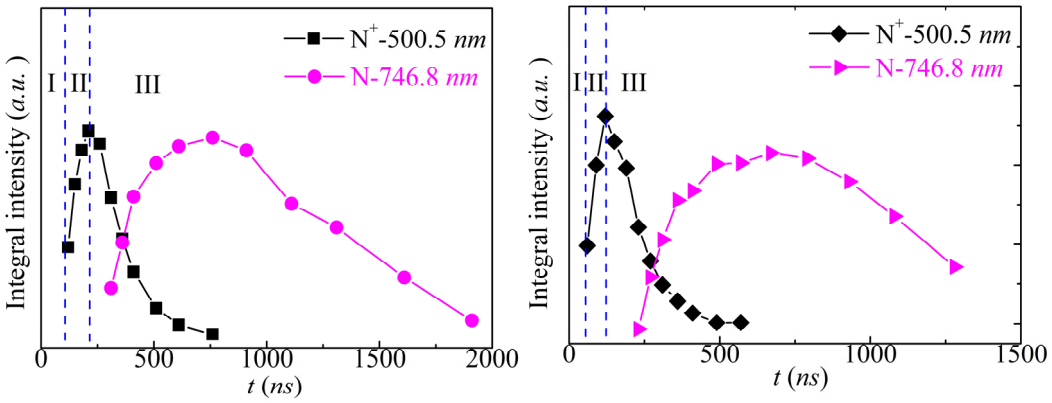

Figure 3 Delay time dependence of the integral intensity for the spectral peaks of N^+ ions and N atoms within the plasma generated by laser irradiation at the niobium surface. The laser irradiation energy density 20 J/cm^2 for the left figure and 10.4 J/cm^2 for the right figure.

Figure 1 shows that the spectral peaks of the N^+ ions and N atoms in the plasma are characteristic and their half-width decreases as the delay time increases. The half width

may be dominated by the local electric field and the related Stark broadening effect which is commonly present in the plasma [21]. When the laser irradiation energy density dropped to 10.4 J/cm^2, the spectral peaks of the plasma were shown in Figure 2. It indicates that the spectral peaks versus the delay time exhibits the similar behaviors to those shown in Figure 1. In both Figure 1 and Figure 2, it is noted that the central wavelength of all the spectral peaks of the N^+ ions and N atoms does not alter with the delay time, despite the dramatic variations in the density and temperature of the plasma as the plasma evolves.

The delay time dependence of the integral intensity for the typical spectral peaks of the N^+ ions and N atoms were shown in Figure 3. It demonstrates that the plasma may undergo several stages labeled by the dashed lines in the figure. In stage I, the plasma may remain in the high temperature and high density state, making the plasma opaque for the measured spectral peaks. As a result, there is no observably spectral peaks. As the plasma expands in stage II, the density and temperature may gradually decline and the plasma may progressively become transparent, leading to an enhanced intensity of the spectral peaks. Interestingly, the spectral peaks of the N^+ ions can be observed, but no spectral peaks of the N atoms can be observed in stage II, indicating that the N element exists as N^+ ions rather than the N atoms in the stage. As the plasma evolves further and enters stage III, the intensity of the spectral peaks of the N^+ ions gradually decreases but that of the N atoms gradually increases with the delay time. The phenomena may be caused by the inherent physical process that a large number of N^+ ions and ionized electrons recombine to form the N atoms [20].

Besides the LIBS, other physical properties such as the temperature and the density of the plasma should be assessed. The temperature and the density are important physical properties of the plasma and they gradually decrease as the plasma expands with the time. Based on the simulation work [22, 23], when the laser illuminates on the metals with the irradiation energy density 10.4 J/cm^2, the typical temperature and density of the plasma may approximate 1 eV and 10^{27} /m^3, respectively.

According to the experimental results, two problems emerge for the conventional plasma theory. First, the LIBS of the plasma indicates that the N atoms, with an ionization energy 14.5 eV, can be totally ionized to the N^+ ions in the plasma during stage II. However, using the Saha equation and the IPD models, *e.g.*, SP model and EK model which were widely used to calculate IPD and the ionization degree [6, 7, 13, 14, 15], no more than two percent of the N atoms can be ionized to the N^+ ions. In other words, the total ionization of N atoms cannot be explained by the conventional theory. Second, the experimental spectra in this work and previous research [12, 13, 15, 17, 18] demonstrated that the central wavelength of the spectral peaks do not vary in different states of the plasma. It means that the energy levels of the bound electrons do not alter with plasma evolution. However, the conventional plasma theory, considering the screening effect and the scattering between the bound electrons and ionized electrons, would definitely yield a shifted energy level for the bound electrons [2, 4, 5, 9, 10, 19]. The fixed central wavelength of the spectral peaks in different states of the plasma cannot be understood by the conventional plasma theory.

To address these problems, the conventional plasma theory should be further

developed. Considering the ionized electrons in the equilibrium state, any plasma inhomogeneity can induce a macro-electric field which may obey *Yuheng Zhang* equation [24, 25],

$$\nabla E_F(\vec{r}) = e\vec{E}(\vec{r}) \tag{1}$$

where $E_F(r)$ is the position-dependent electron chemical potential (ECP), e is the electron charge, and $E(r)$ is the macro-electric field within the plasma. If the plasma exhibits non-uniformity in density, the spatial gradient of the electron density will engender a diffusion current density according to the Fick's law. Concurrently, upon attainment of the electron equilibrium state, an electric field will be induced, as described by equation (1), which in turn can result in a drift current density. Hence, the total current density is the summation of both the diffusion current density and the drift current density [26, 27],

$$j_t = \sigma_e \vec{E}(\vec{r}) - eD_e \nabla n_e(\vec{r}) \tag{2}$$

where j_t represents the total electron current density, $n_e(r)$ denotes the macroscopically average density of the ionized electron over a spatial scale much larger than the atomic scale, D_e signifies the diffusion coefficient of the ionized electrons, $\sigma_e = en_e\mu_e$ is the electrical conductivity where it is assumed that the ionized electrons may dominate the electrical conductivity owing to their much smaller masses than ions, μ_e is the mobility of the ionized electrons, and $E(r)$ refers to the macro-electric field within the plasma.

3.1 Theoretical treatment for electrons in plane wave functions

3.1.1 Mechanical-electric coupling

Analogous to the case of the metals [24, 25, 28, 29], the mechanical-electric coupling

(MEC) of the plasma can be articulated by

$$C_{m-e} = \frac{dE_F}{d\ln V(\vec{r})} \tag{3}$$

where $V(r)$ is the position-dependent volume of the plasma, and it fulfills the relationship $n_e(r)V(r)=N_e$, with N_e representing the total number of ionized electrons in the plasma. Using the MEC concept, the diffusion relation for the ionized electrons in the plasma can be derived by setting the total electron current density to zero in equation (2)

$$\frac{D_e}{u_e} = \frac{C_{m-e}}{-e} \tag{4}$$

Based on the Drude model for the ionized electrons in a plasma [1], the mobility of the electron, denoted as u_e, is characterized by the relationship $u_e=e\tau_e/m_e$, where τ_e is the relaxation time. So the diffusion coefficient of the ionized electrons can be ascertained in terms of the above equation

$$D_e = -\frac{\tau_e C_{m-e}}{m_e} \tag{5}$$

As is seen, the diffusion coefficient appears to be proportional to the product of the relaxation time and the MEC. It is different from the conventional result of the diffusion coefficient $D_e= vl/3$ [1] where v, $l=v\tau_e$ represent the mean velocity and mean free path of the ionized electron, respectively.

Upon attainment of electrical equilibrium state for the plasma, the net electron current will approach zero, as delineated by the subsequent relationship,

$$0 = en_e(\vec{r})u_e\vec{E}(\vec{r}) - eD_e\nabla n_e(\vec{r})$$

Using equation (4) in conjunction with the definition of the electrostatic potential φ,

where $E(\vec{r}) = -\nabla\varphi(\vec{r})$, the distribution of the ionized electron $n_e(r)$ can be derived as follows

$$n_e(r) = n_{0e} e^{e\varphi(r)/C_{m-e}} \tag{6}$$

where $n_{0e}(r)$ denotes the initial density of the ionized electrons. In contrast to the conventional result presented in various textbooks [30, 31], the difference may stem from the fact that the term $-C_{m-e}$ supersedes the statistically thermal energy $k_B T$. And it is the same difference that appears between the classical Einstein diffusion relation and the diffusion relation depicted in equation (4).

3.1.2 Debye length

In order to examine the Debye length of the plasma utilizing the MEC, Maxwell equations and *Yuheng Zhang* equation can be employed. And the following relationship can be derived

$$\nabla^2 E_F(\vec{r}) = \frac{e^2}{\varepsilon_0}\left[n_e(\vec{r}) - Z\delta(\vec{r})\right] \tag{7}$$

where Z denotes the valence of an ion, ε_0 signifies the vacuum permittivity. Performing a Taylor expansion of the ECP with respect to the ionized electron density yields

$$\frac{dE_F(\vec{r})}{dn_e(\vec{r})}\nabla^2 n_e(\vec{r}) + \frac{d^2 E_F(\vec{r})}{dn_e^2(\vec{r})}\left[\nabla n_e(\vec{r})\right]^2 = \frac{e^2}{\varepsilon_0}\left[n_e(\vec{r}) - Z_i\delta(\vec{r})\right]$$

The spatial gradient of the ionized electron density $\nabla n_e(\vec{r})$ in a large spatial scale may be a slowly varying function. Hence, the nonlinear term can be ignored, leading to a liner equation

$$\nabla^2 n_e(\vec{r}) \approx \frac{e^2}{\varepsilon_0}\left(\frac{dE_F}{dn_e}\right)^{-1}\left[n_e(\vec{r}) - Z_i\delta(\vec{r})\right] \tag{8}$$

As is shown, the Debye screening wave vector may be given by

$$q_D^2 = \frac{e^2}{\varepsilon_0}\left(\frac{dE_F}{dn_e}\right)^{-1} \tag{9}$$

It is the identical formula shown in the textbook [32], indicating the validity of the derivation here. It is crucial to highlight that the ECP used in equation (8) encompasses both the kinetic energy and the potential energy of the ionized electrons. And it is distinct from the Fermi energy which only contains the kinetic energy of the free electrons, as shown in the textbooks [33, 34]. Using the definition of MEC in equation (3) and the relationship $dE_F/dn_e = -C_{m-e}/n_e$, the Debye screening wave vector may be modified in the following form

$$q_D^2 = \frac{e^2 n_e}{-\varepsilon_0 C_{m-e}} \tag{10}$$

Correspondingly, the Debye length can be given by

$$\lambda_D^2 = \frac{-\varepsilon_0 C_{m-e}}{e^2 n_e} \tag{11}$$

where λ_D represents the Debye length. It indicates that the screening length sensitively depends on the MEC of the plasma, and a small magnitude of the negative MEC may result in a reduced Debye length.

The preceding theoretical discussion has introduced the MEC for the plasma and underscored its important role for various properties of the ionized electrons within the framework of the plane-wave functions.

3.2 Theoretical treatment for electrons in spherical wave functions

3.2.1 Ionization of the atoms and ions

As previously discussed, various experimental results suggests that the energy levels of the bound electrons within the atoms and ions may not be affected by the plasma

environment. It implies that the atomic Coulomb potential for the bound electrons is likely impervious to the Debye screening effect and the plasma environment. In another respect, the ionized electrons may generally undergo a nonzero potential, denoted as ϕ_0. The potential may be important for understanding the plasma and can be regarded as a mean-field outcome of the complex interactions, such as the attraction from the ion cores and the repulsion from other ionized electrons. For the sake of simplicity, the potential ϕ_0 can be treated as a constant. As a result, the total potential governing the ionization of a bound electron is illustrated in Figure 4. In the potential model, the action radius of the atomic Coulomb potential can be defined as the cutoff radius r_0.

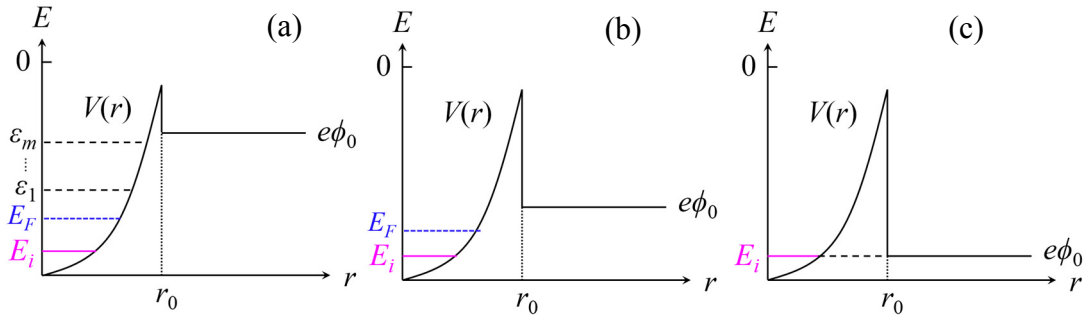

Figure 4 Radius dependence of the potential energy for the electron ionization. The atomic Coulomb potential, denoted as $V(r)$, is operative within the cutoff radius r_0 and the constant potential energy, signified as $e\phi_0$, works outside the radius r_0. (a) the ionization energy levels $\varepsilon_1 \ldots \varepsilon_m$ of the bound electron in the excited states exist below the constant potential energy $e\phi_0$; (b) no ionization energy levels of the bound electron in the excited states exists below potential energy $e\phi_0$; (c) the constant potential energy $e\phi_0$ equals to the ionization energy level E_i of the bound electron in the ground state.

The mathematical form of the potential energy can be written as

$$V_{ep}(r)=\begin{cases}V(\vec{r}),\ r\le r_0\\ e\phi_0,\ r\ge r_0\end{cases} \tag{12}$$

where $V_{ep}(r)$ represents the electron potential energy, $V(r)$ denotes the atomic Coulomb potential and it depends on the configuration of residual bound electrons rather than the ambient plasma environment, r_0 stands for the cutoff radius of the atomic Coulomb potential, $e\phi_0$ signifies the constant potential energy for the ionized electron and it is contingent upon the plasma environment. The state of the ionized electron can be described by the Schrödinger equation in the spherical coordinates,

$$-\frac{\hbar^2}{2m_e}\frac{1}{r^2}\left[\frac{\partial}{\partial r}\left(r^2\frac{\partial}{\partial r}\right)+\frac{1}{\sin\theta}\frac{\partial}{\partial\theta}\left(\sin\theta\frac{\partial}{\partial\theta}\right)+\frac{1}{\sin^2\theta}\frac{\partial^2}{\partial\varphi^2}\right]\psi_f(r,\theta,\varphi)=(E_i-e\phi_0)\psi_f(r,\theta,\varphi)$$

where $\hbar$ denotes the reduced Plank constant, $\psi_f(r, \theta, \varphi)$ stands for the wave function of the ionized electron in the spherical coordinates, E_i signifies the ionization energy level of the bound electron in ground state and $-E_i$ is the related ionization energy. It should be noted that the ionization energy level E_i results from the strong correlation effect of the bound electrons in the ion, and it typically resides significantly higher than the associated bound energy level.

Using the method of separation of variables, the electron wave function can be expressed as $\psi_f(r, \theta, \varphi)=AR(r)Y(\theta, \varphi)$ where $R(r)$ is the radial function and $Y(\theta, \varphi)$ is the spherical harmonics, A is the non-zero normalization coefficient. Consequently, the Schrödinger equation is transformed into the subsequent pair of equations

$$\left[\frac{1}{\sin\theta}\frac{\partial}{\partial\theta}\left(\sin\theta\frac{\partial}{\partial\theta}\right)+\frac{1}{\sin^2\theta}\frac{\partial^2}{\partial\varphi^2}\right]Y(\theta,\varphi)+l(l+1)Y(\theta,\varphi)=0$$

$$\frac{1}{r^2}\frac{\partial}{\partial r}\left(r^2\frac{\partial}{\partial r}\right)R(r)+\frac{2m_e(E_i-e\phi_0)}{\hbar^2}R(r)-\frac{l(l+1)}{r^2}R(r)=0$$

where l represents an integer and it is l=0, 1, 2…

In the scenario where $E_i > e\phi_0$, the partial differential equation can be formulated as

$$\frac{\partial^2 R(r)}{\partial r^2} + \frac{2}{r}\frac{\partial R(r)}{\partial r} + \left[k^2 - \frac{l(l+1)}{r^2}\right] R(r) = 0$$

where the parameter k is defined as $k = \sqrt{2m_e(E_i - e\phi_0)/\hbar^2}$. Its mathematical solution is the spherical Hankel function which describes the radial wave function for the ionized electron propagating away from the atom

$$R(r) = h_l(kr) = -i(-1)^l (kr)^l \left(\frac{1}{kr}\frac{d}{kdr}\right)^l \frac{e^{ikr}}{kr} \tag{13}$$

where the term in the form $(-i)^{l+1}e^{ikr}/kr$ is always present, thereby allowing the subsequent integral to approach an infinite value

$$\int_{r_0}^{\infty} r^2 |R(r)|^2 dr \int_0^{\pi} d\theta \int_0^{2\pi} d\varphi |Y_l(\theta,\varphi)|^2 \to \infty$$

It results in an infinite ratio between the probability of the electron in the ionized state and that in the bound sate. It means that the bound electron with the ionization energy level higher than the potential energy, *i.e.*, $E_i > e\phi_0$, will undergo the complete ionization.

In another scenario where $E_i < e\phi_0$, the partial differential equation of the radial function can be written as

$$\frac{\partial^2 R(r)}{\partial r^2} + \frac{2}{r}\frac{\partial R(r)}{\partial r} + \left[(ik)^2 - \frac{l(l+1)}{r^2}\right] R(r) = 0$$

where the related parameter is $k = \sqrt{2m_e(e\phi_0 - E_i)/\hbar^2}$. The corresponding solution may also be the spherical Hankel function

$$R(r) = h_l(ikr) = -i^l (kr)^l \left(\frac{1}{kr}\frac{d}{kdr}\right)^l \frac{e^{-kr}}{kr} \tag{14}$$

The solution is an attenuation function, indicating that the electron may remain bound even though the wave function has been extended in space.

Combining the aforementioned two scenarios, when the electron potential energy $e\phi_0$ will be continuously reduced to the ionization energy level of the bound electron in ground state, *i.e.*, $e\phi_0=E_i$, the electron will transform from the bound state to the fully ionized state. In other words, an insulator-metal phase transition happens when the electron potential energy $e\phi_0$ crosses the ionization energy level E_i. Therefore, the insulator-metal phase transition can be characterized by the closure of the ionization gap. Furthermore, when the electron potential energy $e\phi_0$ decreases to the value lower than the ionization energy level of the last bound electron during the continuous ionization, the plasma will be considered to be fully ionized.

3.2.2 Distribution function of the ionized electrons

Assuming that the ionized electrons in the plasma are in the *s* state (l=0), the related wave functions are spherically symmetric. So the ionized electron density around a positive ion core can be given by

$$\left|R(r)\right|^2=\frac{1}{(kr)^2}$$

In the *k*-space the ionized electrons are believed to satisfy the famous Maxwell distribution. Therefore, the distribution function for the ionized electrons may be expressed as

$$f_e\left(\vec{k},\vec{r}\right)=A\frac{e^{-\hbar^2k^2/2m_ek_BT}}{(kr)^2}$$

where k is the wave vector, k_B is the Boltzmann constant, T is the temperature of the plasma, and A denotes a pre-factor. By invoking the electron number conservation, the pre-factor A can be determined, and the distribution can be specified as

$$f_e\left(\vec{k},\vec{r}\right)=\frac{Zh}{2\sqrt{2\pi m_e k_B T}}\frac{1}{r_e-r_0}\frac{e^{-\hbar^2k^2/2m_e k_B T}}{\left(kr\right)^2} \tag{15}$$

where Z represents valence of the ion in Wigner-Seitz cell, h signifies the Plank constant, r_e denotes the radius of the Wigner-Seitz cell, and the spin degeneracy factor of 2 has been incorporated. The distribution function in the k-space may be usually utilized and it can be derived by integrating over the spatial coordinates

$$f_e\left(\vec{k}\right)=\frac{2\pi Zh}{\sqrt{2\pi m_e k_B T}}\frac{e^{-\hbar^2k^2/2m_e k_B T}}{k^2} \tag{16}$$

In another respect, the ionized electron density in a Wigner-Seitz cell can also be derived

$$f_e\left(\vec{r}\right)=\frac{Z}{4\pi}\frac{1}{\left(r_e-r_0\right)r^2} \tag{17}$$

3.2.3 Electron heat capacity

Based on the distribution function for the ionized electrons, the average energy of an ionized electron within the plasma is given by

$$\varepsilon_e=e\phi_0+\frac{k_B T}{2} \tag{18}$$

The related heat capacity at constant volume reads

$$c_e=\frac{1}{2}k_B+\frac{e\partial\phi_0}{\partial T} \tag{19}$$

where the first term on the right hand originates from the kinetic energy and it is one third of the conventional value $3k_B/2$. The second term is derived from the potential energy of the ionized electron.

3.2.4 The electron chemical potential

Considering a single-component plasma, the ionization process can be described by

the following transition

$$A_{i-1} \leftrightarrow A_i + e$$

where A_{i-1} represents the ion in ionization state i–1 (possessing i–1 ionized electrons), while A_i denotes the ion in ionization state i (with i ionized electrons), e denotes the ionized electron. Due to the conservation of the electrons during the ionization process, the following relationship may hold true

$$ZN_A = \frac{N_A}{1+e^{(E_i-E_F)/k_BT}} + \sum_{l\geq 1}^{\varepsilon_l<e\phi_0} \frac{N_A}{1+e^{(\varepsilon_l-E_F)/k_BT}} + \frac{4N_A(r_e-r_0)}{(2\pi)^2}\int \frac{d\vec{k}}{k^2}\frac{1}{1+e^{(\varepsilon_{ik}+e\phi_0-E_F)/k_BT}}$$

where E_i denotes the ionization energy level of the bound electron in the ground state and it is negative here, ε_l ($l \geqslant 1$) stands for the ionization energy levels of the bound electron in the excited states and they are also negative, ε_k signifies the positive kinetic energy of the ionized electron and it is $\varepsilon_k=\hbar^2k^2/2m_e$, E_F is the ECP, N_A is the total number of atoms and ions within the plasma, T represents the uniform temperature of the plasma, ϕ_0 is constant potential of the ionized electron in the free space and it generally depends on the electron density and the temperature.

The line density of the ionized electron in the Wigner-Seitz cell may be

$$f_{le} = \frac{4}{(2\pi)^2}\int d\vec{k}\frac{1}{1+e^{(\varepsilon_{ik}+e\phi_0-E_F)/k_BT}}\frac{1}{k^2}$$

where f_{le} signifies the average line density of the ionized electrons in a Wigner-Seitz cell. In the case that the physical parameters fulfill the condition $4(r_e - r_0)(2\pi m_e k_B T/h^2)^{1/2} \gg 1$, the ECP in the above equation can be obtained in terms of simple calculations

$$E_F = e\phi_0 - k_B T \ln\left[\frac{4}{f_{le}}\frac{\left(2\pi m_e k_B T\right)^{1/2}}{h}\right] \tag{20}$$

In the case that Z=1, the ECP can be expressed as

$$E_F \approx \frac{E_i + e\phi_0}{2} - \frac{k_B T}{2}\left\{\ln\left[4\left(r_e - r_0\right)\frac{\left(2\pi m_e k_B T\right)^{1/2}}{h}\right] + \ln\left[1 + \frac{1}{4\left(r_e - r_0\right)}\frac{h}{\left(2\pi m_e k_B T\right)^{1/2}}\sum_{l\geq 1}^{\varepsilon_l < e\phi_0} e^{\left(e\phi_0 - \varepsilon_l\right)/k_B T}\right]\right\}$$

It may indicate that the excitation states of the bound electrons would lead to the reduction of the ECP which may reduce the ionization degree of the bound electrons. If there is no excitation state between ionization energy level E_i and the potential energy $e\phi_0$, the ECP can be simplified to be

$$E_F = \frac{e\phi_0 + E_i}{2} - \frac{k_B T}{2}\ln\left[4\left(r_e - r_0\right)\frac{\left(2\pi m_e k_B T\right)^{1/2}}{h}\right] \tag{21}$$

Consequently, the MEC can be expressed as

$$C_{m-e} = \frac{1}{2}\left[\frac{e\partial\phi_0}{\partial \ln V} - \frac{k_B T}{3}\frac{r_e}{r_e - r_0}\right] \tag{22}$$

In the case that $Z \geqslant 2$, *i.e.*, two or more electrons will be ionized for every atom, the ECP can be approximated by

$$E_F \approx e\phi_0 - k_B T\left\{\ln\left[\frac{4\left(r_e - r_0\right)}{Z-1}\frac{\left(2\pi m_e k_B T\right)^{1/2}}{h}\right] + \ln\left[1 + \frac{1}{4\left(r_e - r_0\right)}\frac{h}{\left(2\pi m_e k_B T\right)^{1/2}}\sum_{l\geq 1}^{\varepsilon_l < e\phi_0} e^{\left(e\phi_0 - \varepsilon_l\right)/k_B T}\right]\right\}$$

In the absence of the excitation states, the ECP may be simplified to

$$E_F \approx e\phi_0 - k_B T \ln\left[\frac{4\left(r_e - r_0\right)}{Z-1}\frac{\left(2\pi m_e k_B T\right)^{1/2}}{h}\right] \tag{23}$$

Thus, the MEC can be formulated as

$$C_{m-e} = \frac{e\partial\phi_0}{\partial \ln V} - \frac{k_B T}{3}\frac{r_e}{r_e - r_0} \tag{24}$$

To be summarized, the general MEC can be articulated as

$$C_{m-e}=\begin{cases}\dfrac{1}{2}\left[\dfrac{e\partial\phi_0}{\partial\ln V}-\dfrac{k_BT}{3}\dfrac{r_e}{r_e-r_0}\right]; for\ \ Z=1\\ \dfrac{e\partial\phi_0}{\partial\ln V}-\dfrac{k_BT}{3}\dfrac{r_e}{r_e-r_0}; for\ \ Z\geq 2\end{cases} \tag{25}$$

Using the line density of the ionized electrons in a Wigner-Seitz cell, the conventional Saha equation may be modified to be

$$\frac{n_i f_{le}}{n_{i-1}}=\frac{4\left(2\pi m_e k_B T\right)^{1/2}}{h\left[1+\sum_{l\geq 1}^{\varepsilon_l<e\phi_0} e^{-(\varepsilon_l-E_i)/k_BT}\right]}e^{-(e\phi_0-E_i)/k_BT}$$

where n_i and n_{i-1} represent the number densities of the ions in the ionization state i and i–1, respectively. If there is not any excitation state, the above modified Saha equation may be simplified to

$$\frac{n_i f_{le}}{n_{i-1}}=\frac{4\left(2\pi m_e k_B T\right)^{1/2}}{h}e^{-(e\phi_0-E_i)/k_BT} \tag{26}$$

It reveals that the conventional Saha equation overlooked several critical aspects. First, the derivations of Saha equation did not consider the quantum many-body correlation effect for the electron ionization, so the related quantum degeneracies might be 1 stead of g_i and g_{i+1}. Second, the Saha equation traditionally attributed the reduction of the energy gap to the decrease of the ionization energy $-E_i$, which contradicts with the time-dependent spectroscopy of the ions and atoms in the plasma. Based on the experimental spectroscopy, the energy levels of the bound electrons may not be affected, and the energy gap ε_g may be solely influenced by the variation of the potential energy $e\phi_0$ for the ionized electrons. Third, the Saha equation only considered the ionization of the bound electron at ground state, disregarding the impact of the excitation states on the

ionization. Fourth, the Saha equation treated the ionized electrons as plane waves and used the average spatial density of the ionized electrons, thereby neglecting the possible position-dependent spatial density of the ionized electrons.

3.2.5 Potential energy of the ionized electrons

To determine the potential energy of the ionized electrons, the method of the Wigner-Seitz cell can be employed, a technique widely used in the study of the plasma and the crystalline materials [32, 34]. Under the assumption that the ionized electrons are in the *s* state, *i.e.*, l=0, the related wave-functions are spherically symmetric. As a result, the total Coulomb attraction energy for the ionized electrons within a Wigner-Seitz cell may be given by

$$\varepsilon_a = -\int_{r_0}^{r_e} d\vec{r}\,\frac{Ze^2 f_e(r)}{4\pi\varepsilon_0 r}$$

By performing the straightforward calculations, the analytical result can be derived as

$$\varepsilon_a = -\frac{2Z^2 Ry}{(r_u - r_d)}\ln\frac{r_u}{r_d} \tag{27}$$

where *Ry* represents the Rydberg, defined as $Ry = e^2/8\pi\varepsilon_0 a_B = 13.6\ eV$, a_B signifies the Bohr radius, and the dimensionless parameters are r_u=r_e/a_B, r_d=r_0/a_B.

The direct Coulomb repulsion energy between the ionized electrons within the same Wigner-Seitz cell can be expressed as

$$\varepsilon_C = \frac{1}{2}\int_{r_0}^{r_e} d\vec{r}_1 \int_{r_0}^{r_e} d\vec{r}_2\,\frac{e^2 f_e(r_1) f_e(r_2)}{4\pi\varepsilon_0 |\vec{r}_1 - \vec{r}_2|}$$

In terms of calculations, it may be depicted as

$$\varepsilon_C = \frac{2Z^2 Ry}{(r_u - r_d)}\left[1 - \frac{r_d}{r_u - r_d}\ln\frac{r_u}{r_d}\right] \tag{28}$$

where the cutoff radius r_0 is very important and it may be considered as the effective Bohr radius which can be delineated using the ionization energy [2],

$$\frac{Ze^2}{8\pi\varepsilon_0 r_0} = \left|E_i\right|$$

Therefore, the reduced cutoff radius r_d is

$$r_d = \frac{ZRy}{\left|E_i\right|} \tag{29}$$

And another reduced radius r_u can be given according to the average volume of the ions,

$$r_u = \left(\frac{4\pi}{3} a_B^3 n_A\right)^{-1/3} \tag{30}$$

Besides the attraction energy and the Coulomb repulsion energy, the exchange energy among the ionized electrons within the same Wigner-Seitz cell must also be taken into account. The ionized electrons may not exhibit the local magnetic moment at the ion site. Hence, the ionized electrons may present the singlet state. Following the computational procedures outlined in the textbook [32], the exchange energy for the spin singlet state can be given by

$$\varepsilon_{exch-s} = \frac{1}{2}\int \frac{d\vec{k}d\vec{r}}{(2\pi)^3}\frac{d\vec{k}'d\vec{r}'}{(2\pi)^3} f_e\left(\vec{k},\vec{r}\right) f_e\left(\vec{k}',\vec{r}'\right) e^{i(k-k')(r-r')} \frac{e^2}{4\pi\varepsilon_0\left|\vec{r}-\vec{r}'\right|}$$

Through the mathematical derivations, the exchange energy can be obtained

$$\varepsilon_{exch-s} = \frac{2Z^2 Ry}{\left(r_u - r_d\right)}\frac{\sqrt{\pi}}{2t}\int_{r_d}^{r_u} dr \frac{Erf\left(t'\right)}{r} \tag{31}$$

where t , t' are the dimensionless parameters defined as $t = (m_e k_B T a_B^2/\hbar^2)^{1/2}(r_u - r_d)$ and $t' = (m_e k_B T a_B^2/\hbar^2)^{1/2}(r - r_d)$, respectively, *Erf*(*t*) signifies the error function given by $Erf(t) = \frac{2}{\sqrt{\pi}}\int_0^t e^{-x^2} dx$.

Moreover, the interaction between the adjacent ions should be taken into account

when considering the potential energy of the ionized electrons. The Coulomb attraction energy between the ionized electrons and the nearest-neighboring ion core can be determined using the ionized electron distribution function and it is given be

$$\varepsilon_a' = -\int_{r_0}^{r_e} d\vec{r}\,\frac{\left(Z-1+\alpha_{Ze}\right)e^2 f_e\left(r\right)}{4\pi\varepsilon_0\left|\vec{r}-\vec{R}\right|}$$

where $\vec{R}$ represents the position vector of the nearest-neighboring ion with the magnitude $2r_e$. Substitution of equation (17) into the above equation will yield

$$\varepsilon_a' = -\frac{Z\left(Z-1+\alpha_{Ze}\right)e^2}{4\pi\varepsilon_0\left(2r_e\right)} \tag{32}$$

where $2r_e$ denotes the distance between the two nearest-neighboring ions, the parameter α_{Ze} represents the ionization degree for the ion with Z ionized electrons, and $Z-1+\alpha_{Ze}$ signifies the average ionized electron per atom. The average Coulomb repulsion energy between the ionized electrons in the ion and those in the nearest-neighboring ion may be

$$\varepsilon_C' = \frac{1}{2}\int_{r_0}^{r_e} d\vec{r}\int_{r_0}^{r_e} d\vec{r}'\,\frac{\left(Z-1+\alpha_{Ze}\right)}{Z}\,\frac{e^2 f_e\left(r\right)f_e\left(r'\right)}{4\pi\varepsilon_0\left|\vec{r}-\vec{r}'-\vec{R}\right|}$$

where the pre-factor 1/2 is due to the fact that the ionized electrons within the two ions share the Coulomb repulsion energy. Insertion of equation (17) will give the result

$$\varepsilon_C' = \frac{1}{2}\frac{Z\left(Z-1+\alpha_{Ze}\right)e^2}{4\pi\varepsilon_0\left(2r_e\right)} \tag{33}$$

For an ion with the coordination number z_1, the energy contributed by the neighboring ions may read

$$\varepsilon_a' + \varepsilon_C' = -\frac{z_1}{2}\frac{Z\left(Z-1+\alpha_{Ze}\right)e^2}{4\pi\varepsilon_0\left(2r_e\right)}$$

As a result, the average potential energy for an ionized electron can be articulated by

$$e\phi_0 = \frac{\varepsilon_a + \varepsilon_C + \varepsilon_{exch-s} + \varepsilon'_a + \varepsilon'_C}{Z}$$

Substitution of the related energies into the above equation will yield

$$e\phi_0 = -\frac{2ZRy}{(r_u - r_d)}\left[\frac{r_u}{r_u - r_d}\ln\frac{r_u}{r_d} - 1 - \frac{\sqrt{\pi}}{2t}\int_{r_d}^{r_u} dr\frac{Erf(t')}{r}\right] - \frac{z_1}{2}\frac{(Z - 1 + \alpha_{Ze})Ry}{r_u} \quad (34)$$

It is the IPD model for the single-component plasma in the work. To examine the applicability of the model, a comparison between the model and the experimental results is necessary. Using the model along with the experimental data of the aluminum plasma [12], the calculated IPD values for the aluminum ions and the experimental counterpart were shown in Figure 5. As is shown, the IPD values given by the model may agree with the experimental values better than those obtained from the EK model and SP model.

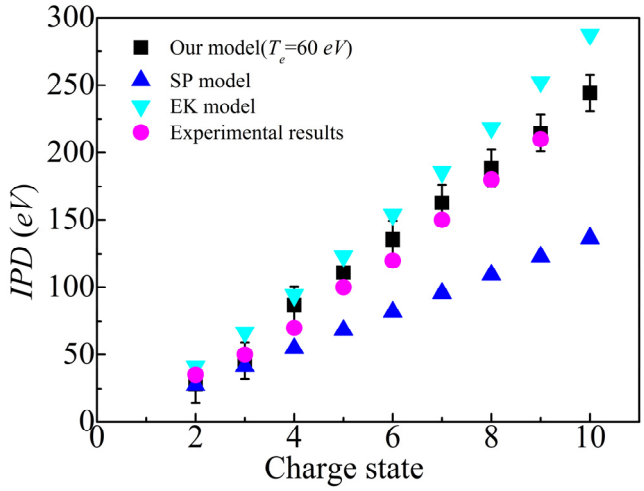

Figure 5. Charge state dependence of the experimental ionization potential depression (IPD) values [12] and those obtained by SP model, EK model and our model for the aluminum ions in the plasma with the solid density 2.7 g/cm^3.

On another hand, it is necessary to further investigate whether the model can account for the total ionization of N atoms during the laser nitriding process. As previously

stated, the experimental spectroscopy demonstrated that all the N atoms can be ionized to be the N^+ ions during stage II of the laser-nitriding process. It can be implied that the Nb atoms can be ionized to be the Nb^{2+} ions whose second ionization energy (14.3 *eV*) is comparable to the first ionization energy (14.5 *eV*) of the N atoms. Given the situation where the a N^+ ion is surrounded by both the Nb^{2+} and N^+ ions within the plasma, the potential energy for the ionized electron in the N^+ ion may be modified to be

$$e\phi_0 = -\frac{2Ry}{\left(r_{u1}-r_{d1}\right)}\left[\frac{r_{u1}}{r_{u1}-r_{d1}}\ln\frac{r_{u1}}{r_{d1}}-1-\frac{\sqrt{\pi}}{2t}\int_{r_{d1}}^{r_{u1}}dr\frac{Erf\left(t'\right)}{r}\right]-\frac{2z_1Ry}{r_{u1}+r_{u2}}-\frac{z_1'Ry}{\sqrt{2}\left(r_{u1}+r_{u2}\right)} \quad (35)$$

where r_{d1} signifies the reduced cutoff radius for the N^+ ion, z_1 and z'_1 represent the number of the nearest-neighboring Nb^{2+} ions and N^+ ions around a N^+ ion, r_{u1} and r_{u2} correspond to the reduced radius of the N^+ ions and the Nb^{2+} ions, respectively. They must satisfy the following relation for the dual-component plasma

$$\frac{4\pi}{3}a_B^3r_{u1}^3n_{A1}+\frac{4\pi}{3}a_B^3r_{u2}^3n_{A2}=1 \quad (36)$$

where n_{A1} and n_{A2} represent the number density of the N^+ ions and the Nb^{2+} ions within the plasma, respectively. For the uniform plasma, the ionized electrons in the different ions may undergo the same potential energy. Therefore, the potential energy for the ionized electron in the Nb^{2+} ion can be expressed in an analogous manner

$$e\phi_0 = -\frac{4Ry}{\left(r_{u2}-r_{d2}\right)}\left[\frac{r_{u2}}{r_{u2}-r_{d2}}\ln\frac{r_{u2}}{r_{d2}}-1-\frac{\sqrt{\pi}}{2t}\int_{r_{d2}}^{r_{u2}}dr\frac{Erf\left(t'\right)}{r}\right]-\frac{z_1Ry}{r_{u1}+r_{u2}}-\frac{z_1'\sqrt{2}Ry}{\left(r_{u1}+r_{u2}\right)} \quad (37)$$

where r_{d2} denotes the reduced cutoff radius for the Nb^{2+} ion, z_1 and z'_1 are the numbers of the nearest-neighboring N^+ ions and Nb^{2+} ions around a Nb^{2+} ion, respectively, and they depend on the structure of the plasma. Although the exact structure of the dual-component plasma remains unknown, an assumption can be made that the Nb^{2+}, N^+

ions construct a simple cubic lattice, with alternating occupancy of the lattice sites. Under the assumption, the important numbers are z_1=6, z'_1=12. Other important parameters such as the temperature and the density of the plasma can be estimated by the relevant simulation. According to the simulation work [22, 23, 35], the typical temperature and density of the plasma created by laser illumination on metals with the irradiation energy density 10.4 J/cm^2 may be approximated as 1 eV and 10^{27} $/m^3$, respectively. By substituting the experimental parameters into the conventional EK model and SP model, the density-dependent IPD values were obtained and were displayed in Figure 6. As indicated, the IPD for the N atoms at the experimental density may be less than 5 eV. Such a small IPD suggests that only a minor fraction of N atoms will be ionized, which is inconsistent with the experimental spectroscopy in the work. On the contrary, the potential energy of the ionized electron in the N^+ ion is found to reach a value of –17 eV based on equations (35) (36) and (37). In other words, the related IPD is 17 eV which exceeds the first ionization energy and can lead to the complete ionization of the N atoms, as agrees with the experimental spectroscopy shown in Figure 1, 2 and 3.

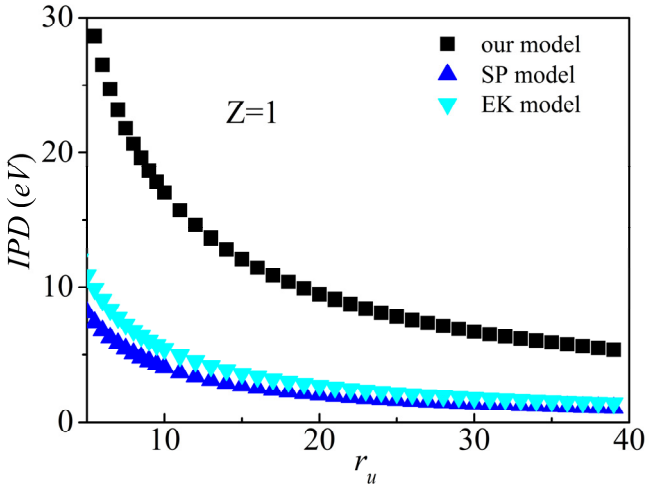

Figure 6. Reduced radius r_u (defined in the paper) dependence of ionization potential depression (IPD) for the N atoms in the plasma during the laser nitriding process. The temperature of the plasma was assumed to be 1 eV.

3.2.6 Equation of state

To study the related pressure of the ionized electrons in the plasma, the canonical partition function can be utilized [36] and it is given by

$$Z_e = \sum_k 2e^{-\beta(e\phi_0+\varepsilon_{ik})}$$

where the factor 2 takes the spin degeneracy into account, the parameter β is defined as $\beta=1/k_BT$. Performing the integration of the partition function will yield

$$Z_e = 4(r_e - r_0)\left(\frac{2\pi m_e k_B T}{h^2}\right)^{1/2} e^{-\beta e\phi_0}$$

As a result, the electron pressure can read

$$p_e = \frac{N_e \partial \ln Z_e}{\beta \partial V} = \begin{cases} -2n_A\alpha_e C_{m-e} & ;\, for\ \mathrm{Z}=1 \\ -n_A\left(Z-1+\alpha_{Ze}\right)C_{m-e} & ;\, for\ Z \geq 2 \end{cases} \tag{38}$$

Insertion of the expression for the MEC may give birth to the general formula

$$p_e = -n_A\left(Z-1+\alpha_{Ze}\right)\left[\frac{e\partial\phi_0}{\partial \ln V} - \frac{k_BT}{3}\frac{r_u}{r_u - r_d}\right] \tag{39}$$

As demonstrated, the electron pressure is sensitively dependent on the ionization degree, the MEC and the total density of the ions and the atoms within the plasma. The sign of MEC may dictate the sign of the electron pressure. If the MEC is positive, the ionized electrons will display a negative pressure. Conversely, if the MEC is negative, the ionized electrons will exhibit a positive pressure.

The canonical partition function for the ions and atoms within the plasma can be

expressed in the similar manner

$$Z_A = \sum_k e^{-\beta\varepsilon_k - \beta z_1 (Z-1+\alpha_{Ze})^2 Ry/2r_u}$$

where Z_A denotes the canonical partition function for the ions and atoms within the plasma, the second term in the exponential function represents the average Coulomb repulsion between the ion core and the nearest-neighboring ion cores. The integration can be carried out to obtain the result

$$Z_A = V\left(\frac{2\pi m_{ion} k_B T}{h^2}\right)^{3/2} e^{-\beta z_1 (Z-1+\alpha_{Ze})^2 Ry/2r_u}$$

Consequently, the pressure can be formulated as

$$p_A = n_A k_B T + n_A \frac{z_1 \left(Z-1+\alpha_{Ze}\right)^2 Ry}{6r_u}$$

The total pressure of the plasma may be the summation of the electron pressure and the ion pressure

$$p_{tot} = p_A + p_e$$

where p_{tot} is the total pressure of the plasma. Substituting the relevant expressions for the pressures yields

$$p_{tot} = n_A k_B T - n_A \left(Z-1+\alpha_{Ze}\right)\left[\frac{e\partial\phi_0}{\partial \ln V} - \frac{k_B T}{3}\frac{r_u}{r_u - r_d}\right] + \frac{n_A z_1 \left(Z-1+\alpha_{Ze}\right)^2 Ry}{6r_u}$$

It indicates that the total pressure of the partially ionized plasma may depend on the temperature, the MEC, the ionization degree and the total density of the neutral atoms and the positive ions. Insertion of the expression for the potential energy of ionized electrons will give rise to the following result

$$p_{tot} = n_A k_B T\left[1+\frac{\left(Z-1+\alpha_{Ze}\right)}{3}\frac{r_u}{r_u - r_d}\right] - \frac{2n_A Z\left(Z-1+\alpha_{Ze}\right) r_u Ry}{3\left(r_u - r_d\right)^2}\left[\frac{r_u + r_d}{r_u - r_d}\ln\frac{r_u}{r_d} - 2 - \frac{\sqrt{\pi}}{t}\int_{r_d}^{r_u} dr \frac{Erf(t')}{r} + \frac{\sqrt{\pi}}{2t}\frac{r_u - r_d}{r_u} Erf(t)\right] \quad (40)$$

where the contribution of the Coulomb repulsion energy between the ion core and the nearest-neighboring ion cores may be cancelled by the related energy between the ionized electrons and the nearest-neighboring ions. As a result, the total pressure does not explicitly contain the contribution from the neighboring ions. But the total pressure does implicitly contain a contribution from the nearest-neighboring ions, which can influence the ionization degree and the number of ionized electrons.

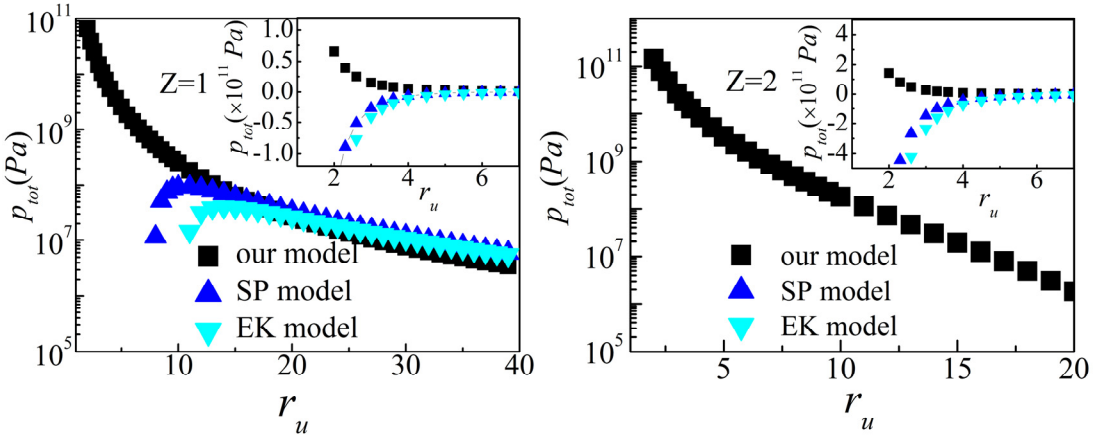

Figure 7 Reduced radius r_u (defined in the paper) dependence of the pressure for the plasma. Black squared represent the results calculated by our model, the blue triangles and the inverted cyan triangles denote the results based on SP model and EK models, respectively. The charge state Z=1 for left diagram for and Z=2 for right diagram. The insets present the related diagram in linear scale.

To evaluate the validity of the equation of state presented in equation (40), it is essential to compare it with other models and the related experimental data. The models like the EK and SP models often concentrate on the IPD, but they frequently overlook whether the proposed model can provide a rational equation of state for the plasma [6, 7, 8]. Using the EK model and SP model models, it may be predicted that the plasma sometimes exhibits the negative pressure shown in Figure 7. The prediction may be

unreasonable and at odds with the positive pressure observed by the experiments [37]. To be contrast, our model can give the positive pressure for the equation of state, as presented in Figure 7. The more careful comparison with experimental data was shown in Figure 8. According to the experimental conditions [37], the IPD for the Ni plasma can be estimated in terms of our model and may surpass the second ionization energy (18.2 eV) of the Ni atoms, thereby enabling the plasma exist in the charge state Z=2 under the experimental conditions. Thereafter, the pressure of the plasma can be obtained by means of the equation (40), as shown in Figure 8. It indicated that the plasma pressure calculated by our model is much smaller than that obtained by the ideal gas model and may agree with the experimental observations.

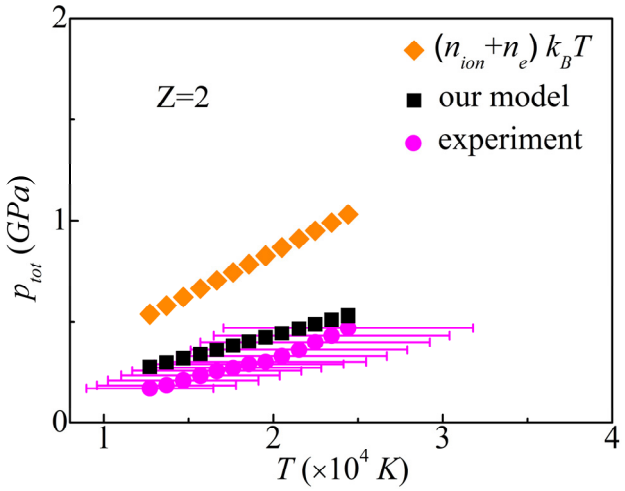

Figure 8. Temperature dependence of the pressure for the single-component (nickel Ni) plasma with the density 0.1 g/cm^3. Orange diamonds, black squared give equation of state for the plasma with charge state Z=2 based on the ideal gas model and our model, respectively. The magenta circled with erro bars denote the experimental observations [37].

4. Conclusion

In summary, the MEC and the IPD for the plasma were investigated from both the experimental and theoretical aspects in the work. The concept of MEC was proposed for the plasma in the work. It was revealed that the MEC may be of paramouont importance and may dominate various physical properties of the plasma such as the diffusion relation of ionized electrons, the Debye screening and the ionzied electron pressure. Furthermore, a model for the IPD was proposed based on the sperically symmetric wave functions for the ionzied electrons within the plasma. The model was found to agree with both the experimental spectroscopy and the experimental IPD for the ions with different charge states. Combination of the MEC and the IPD model may give rise to the equation of state for the plasma, which may be in accord with the experimental observations. Above all, the proposed MEC and IPD model may be vital for people understanding the ionization process and multi-physical properties of the plasma.

Acknowledgement

The author thanks Yu Zhu for his help in the experiments.

Reference

[1]Shalom Eliezer, The Interaction of High-Power Lasers with Plasmas, First edition, Bristol and Philadelphia: Institute of Physics Publishing, 2002, pp. 14-27.

[2] Setsuo Ichimaru, Statistical Plasma Physics (Volume II: Condensed Plasmas), CRC press & Taylor Francis Group, Boca Raton, 2004, pp.198-203.

[3] Alexander Piel, Plasma Physics: An Introduction to Laboratory, Space, and Fusion Plasmas, Second Edition, Springer International Publishing AG, Cham, Switzerland, 2017, pp. 32-34.

[4] Werner Ebeling, Andreas Förster, Vladimir E. Fortov, Viktor K. Gryaznov, Aleksandr Ya. Polishchuk, Thermophysical Properties of Hot Dense Plasmas, B. G. Teubner Verlagsgesellschaft Stuttgart Leipzig 1991, pp.50-57.

[5] Shalom Eliezer, Ajoy Ghatak, Heinrich Hora, Fundamentals of Equations of State, World Scientific Publishing Co. Pte. Ltd., Singapore, 2002, pp.86-103.

[6] G. Ecker; W. Kröll, Lowering of the Ionization Energy for a Plasma in Thermodynamic Equilibrium, Phys. Fluids V.**6**, 62–69 (1963). https://doi.org/10.1063/1.1724509

[7] John C. Stewart, Kedar D. Pyatt, JR., Lowering of Ionization Potential in Plasmas, Astrophys. J. V.**144**, 1203-1211(1966).

[8] Röpke, G., Blaschke, D., Döppner, T., Lin, C., Kraeft, W. D., Redmer, R., & Reinholz, H. Ionization potential depression and Pauli blocking in degenerate plasmas at extreme densities. Physical Review E, **99**(3), 033201(2019).

[9] Zeng, J., Li, Y., Hou, Y., Gao, C., Yuan, J. Ionization potential depression and

ionization balance in dense carbon plasma under solar and stellar interior conditions. Astronomy & Astrophysics, **644**, A92(2020).

[10] Jin, R., Abdullah, M. M., Jurek, Z., Santra, R., Son, S. K. Transient ionization potential depression in nonthermal dense plasmas at high x-ray intensity. Physical Review E, **103**(2), 023203 (2021).

[11] Xiaolei Zan, Chengliang Lin,,Yong Hou, Jianmin Yuan, Local field correction to ionization potential depression of ions in warm or hot dense matter, Physical Review E, **104**, 025203 (2021).

[12] O. Ciricosta , S.M. Vinko, B. Barbrel, D.S. Rackstraw , T.R. Preston, T. Burian, J. Chalupsky, B.I. Cho, H.-K. Chung, G.L. Dakovski, K. Engelhorn, V. Ha´jkova´, P. Heimann, M. Holmes, L. Juha, J. Krzywinski, R.W. Lee, S. Toleikis, J.J. Turner, U. Zastrau, J.S. Wark, Measurements of continuum lowering in solid-density plasmas created from elements and compounds, Nature Communications, **7**:11713 (2016). DOI: 10.1038/ncomms11713

[13] O. Ciricosta, S. M. Vinko, H.-K. Chung, B.-I. Cho, C. R. D. Brown, T. Burian, J. Chalupsky´, 5 K. Engelhorn, R. W. Falcone, C. Graves, V. Ha´jkova´, A. Higginbotham, L. Juha, J. Krzywinski, H.J. Lee, M. Messerschmidt, C. D. Murphy, Y. Ping, D. S. Rackstraw, A. Scherz, W. Schlotter, S. Toleikis, J.J. Turner, L. Vysin, T. Wang, B. Wu, U. Zastrau, D. Zhu, R. W. Lee, P. Heimann, B. Nagler, and J. S. Wark, Direct Measurements of the Ionization Potential Depression in a Dense Plasma, Phys. Rev. Lett. V. **109**, 065002(1-4) (2012).

[14] Carlos A. Iglesias, Philip A. Sterne, Fluctuations and the ionization potential in

dense plasmas, High Energy Density Physics, V.**9** 103-107 (2013)

[15] D.J. Hoarty, P. Allan, S. F. James, C.R. D. Brown, L. M.R. Hobbs, M. P. Hill, J. W. O. Harris, J. Morton, M. G. Brookes, R. Shepherd, J. Dunn, H. Chen, E. Von Marley, P. Beiersdorfer, H. K. Chung, R. W. Lee, G. Brown, J. Emig, Observations of the Effect of Ionization-Potential Depression in Hot Dense Plasma, Phys. Rev. Lett. V. **110**, 265003 (1-5) (2013).

[16] Yuanjie Huang, Yu Zhu, Yu Zhao, Lingyuan Wu, Li Zhang, Yongqiang Zhang, Jichuan Wu, Fuli Tan, Experimental investigation for pulsed laser nitriding of metals, Optics & Laser Technology V. **157**, 108661(1-6) (2023).

[17] Maijuan Li, Maogen Su , Haoyang Li, Qi Min , Shiquan Cao , Duixiong Sun , Denghong Zhang, Chenzhong Dong, Extreme ultraviolet spectral characteristic analysis of highly charged ions in laserproduced Cu plasmas, Plasma Sci. Technol. V. **25**, 045505 (2023).

[18] Sun, D., Su, M., Dong, C., Wen, G. A comparative study of the laser induced breakdown spectroscopy in single-and collinear double-pulse laser geometry. Plasma Science and Technology, **16**(4), 374(2014).

[19] Li, X., Rosmej, F. B. Analytical approach to level delocalization and line shifts in finite temperature dense plasmas. Physics Letters A, **384**(25), 126478(2020)..

[20] Yu Zhu, Ping-Wei Zhou, Seng-Cheng Zhong, Qi-Xian Peng, Li-Guo Zhu, A multi-spot laser induced breakdown spectroscopy system based on diffraction beam splitter, Rev. Sci. Instrum. **90**, 123105(1-7) (2019). https://doi.org/10.1063/1.5120604

[21] Reinhard Noll, Laser-Induced Breakdown Spectroscopy: Fundamentals and

Applications, first edition, Springer-Verlag Berlin Heidelberg, Germany, 2012, pp.173-183.

[22] Peter Schaaf, Laser nitriding of metals, Progress in Materials Science, V. **47**, 1-161(2002).

[23] Jin-Xin Wang, Shi-Yu Li, Xiong Ran, Yongpan Cheng, and Wei-Cheng Yan, Numerical Simulation of Rapid Nitriding of Aluminum via Pulsed Laser, Ind. Eng. Chem. Res. V.**62**, 6460−6472(2023).

[24] Yuanjie Huang, Strain induced electric effect in condensed matters. J Mater Sci Appl. V. **5**(3):44–57(2019).

[25] Yuanjie Huang, Tangential electrostatic field at metal surfaces, Open Physics, V. 21, 20220270(2023).

[26] Feng Duan, Jin GuoJun. Condensed Matter Physics (Volume I). Beijing: Higher Education Press; 2013. p. 218–9.

[27] Grosso G, Parravicini GP. Solid state physics. First edition. Singapore: Elsevier(Singapore) Pte Ltd; 2006. p. 397, 417, 427–9, 434, 469–71.

[28] Yuanjie Huang, Yuheng Zhang effect: strain-induced electric effect in metals. J Mater Sci Appl. V. **5**(3):58–62(2019).

[29] Yuanjie Huang, Electric features of dislocations and electric force between dislocations. Math. Mech. Solid, **26**(4):616–28(2021).

[30] Paul M. Bellan, Fundamentals of Plasma Physics, First edition, New York: Cambridge University Press, 2006, pp.8.

[31] Alexander Piel, Plasma Physics-An Introduction to Laboratory, Space, and Fusion

Plasma, Second edition, Cham, Switzerland: Springer International Publishing AG, 2017, pp. 36.

[32] Philip Phillips, Advanced Solid State Physics, Westview Press, Boulder, 2003, pp.1-8, pp.35-49, pp. 115-118, pp.187-196.

[33] Gerald D. Mahan, Many-Particle Physics, third edition, Kluwer Academic/Plenum Publishers, New York, 2000, pp. 296-302, pp.499-505, pp. 545-549.

[34] Sang-Kil Son (손상길), Robert Thiele, Zoltan Jurek, Beata Ziaja, Robin Santra, Quantum-Mechanical Calculation of Ionization-Potential Lowering in Dense Plasmas, Phy. Rev. X **4**, 031004(1-14) (2014).

[35] Annemie Bogaerts, Zhaoyang Chen, Renaat Gijbels , Akos Vertes, Laser ablation for analytical sampling: what can we learn from modeling? Spectrochimica Acta Part B **58**, 1867–1893(2003).

[36] Zonghan Lin, Thermodynamics and Statistical Physics, 2007, Beijing: Peking University Press, 1st edition, pp. 312-319, pp. 344-348, pp.533-553.

[37] Clérouin, J., Noiret, P., Blottiau, P., Recoules, V., Siberchicot, B., Renaudin, P., Starrett, C. E. A database for equations of state and resistivities measurements in the warm dense matter regime. Physics of Plasmas, **19**(8) (2012).